MM226 Project Report

Development of open source code and GUI for Eshelby Solution

Ashutosh Gandhe, Vishwam Raval, Vedang Bale, Durgesh Sahane

Guide: M.P. Gururajan

Department of Metallurgical Engineering & Materials Science

Indian Institute of Technology, Bombay

1 Introduction of the Eshelby Problem

Eshelby's inclusion problem refers to a set of problems involving ellipsoidal elastic inclusions in an infinite elastic body. It addresses the question of how an inclusion (a small spherical or elliptical region with different material properties) embedded within a material affects the overall stress and strain fields.

1.1 Inclusion and Eigenstrain

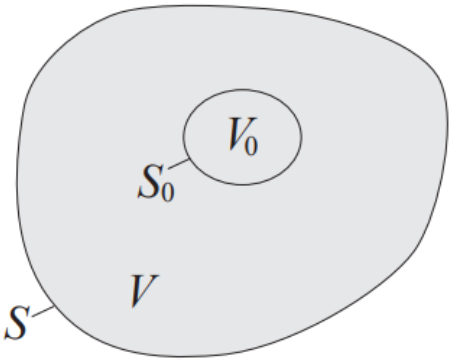

Figure 1: A visual of inclusion and matrix

The above figure shows a solid with volume V and surface S. A subvolumne V_0 having surface S_0 undergoes an elastic deformation. The material inside the subvolume is called *matrix*, and the outside material is called *inclusion*.

2 Mathematical solutions of Isotropic cases

2.1 3D Isotropic Homogeneous Case

Description: An ellipsoidal inclusion Ω has been assumed in an infinitely extending isotropic body. Eigenstrains in the given ellipsoidal domain are assumed to be uniform. Eshelby, through his papers has given the expression for stresses at different exterior and interior points, and an important result is that the strain and stress fields become uniform for the interior points.

2.1.1 Interior Points

Given the dimensions a_1, a_2, a_3 of the inclusion, the procedure is as follows: The solution approach to the problem using the Green's function yields the following integrals:

$$I_i = 2\pi a_1 a_2 a_3 \int_0^\infty \frac{ds}{(a_i^2+s)\Delta(s)} \tag{1}$$

$$I_{ii} = 2\pi a_1 a_2 a_3 \int_0^\infty \frac{ds}{(a_i^2+s)^2\Delta(s)} \tag{2}$$

$$I_{ij} = 2\pi a_1 a_2 a_3 \int_0^\infty \frac{ds}{(a_i^2+s)(a_j^2+s)\Delta(s)} \tag{3}$$

where $\Delta(s) = ((a_1^2+s)(a_2^2+s)(a_3^2+s))^{\frac{1}{2}}$

These integrals can be reduced by using Elliptic integrals, assuming $a_1 > a_2 > a_3$

$$F(\theta,k) = \int_0^\theta \frac{d\omega}{(\sqrt{1-k^2\sin^2\omega})}; E(\theta,k) = \int_0^\theta (\sqrt{1-k^2\sin^2\omega}d\omega) \tag{4}$$

where, $\theta = sin^{-1}(1-\frac{a_3^2}{a_1^2})^{1/2}$, $\quad k = \left(\frac{a_1^2-a_2^2}{a_1^2-a_3^2}\right)^{1/2}$

Using the above elliptic integrals, we get

$$I_1 = \frac{4\pi a_1 a_2 a_3}{(a_1^2 - a_2^2)(a_1^2 - a_3^2)^{\frac{1}{2}}}(F(\theta, k) - E(\theta, k)) \tag{5}$$

$$I_3 = \frac{4\pi a_1 a_2 a_3}{(a_2^2 - a_3^2)(a_1^2 - a_3^2)^{\frac{1}{2}}}\left(\frac{a_2(a_1^2 - a_3^2)^{\frac{1}{2}}}{a_1 a_3} - E(\theta, k)\right) \tag{6}$$

I_2 and I_{12} can be found by the following equations:

$$I_1 + I_2 + I_3 = 4\pi \quad I_{12} = \frac{I_2 - I_1}{(a_1^2 - a_2^2)} \tag{7}$$

Further, I_{11} and I_{13} can be found out by solving the following equations simultaneously:

$$3I_{11} + I_{13} = \frac{4\pi}{a_1^2} - I_{12} \tag{8}$$

$$3a_1^2 I_{11} + a_3^2 I_{13} = 3I_1 - a_2^2 I_{12} \tag{9}$$

Similar cyclic equations can be followed to solve for other $I'_{ij}s$
From the above integrals, the stress for points in the interior of the inclusion can be found out. This stress is uniform due to the uniform strain and isotropic assumption. The formula for the normal and shear stress along X-direction is given by:

$$\begin{aligned}
\frac{\sigma_{11}}{2\mu} = &\left[\frac{a_1^2}{8\pi(1-\nu)}\left(\frac{1-\nu}{1-2\nu}3I_{11} + \frac{\nu}{1-2\nu}(I_{21} + I_{31})\right)\right. \\
&+ \frac{1-2\nu}{8\pi(1-\nu)}\left(\frac{1-\nu}{1-2\nu}I_1 - \frac{\nu}{1-2\nu}(I_2 + I_3)\right) - \left.\frac{1-\nu}{1-2\nu}\right]\epsilon_{11}^* \\
&+ \left[\frac{a_2^2}{8\pi(1-\nu)}\left(\frac{1-\nu}{1-2\nu}I_{12} + \frac{\nu}{1-2\nu}(3I_{22} + I_{32})\right)\right. \\
&- \frac{1-2\nu}{8\pi(1-\nu)}\left(\frac{1-\nu}{1-2\nu}I_1 - \frac{\nu}{1-2\nu}(I_2 - I_3)\right) - \left.\frac{\nu}{1-2\nu}\right]\epsilon_{22}^* \\
&+ \left[\frac{a_3^2}{8\pi(1-\nu)}\left(\frac{1-\nu}{1-2\nu}I_{13} + \frac{\nu}{1-2\nu}(3I_{33} + I_{23})\right)\right. \\
&- \frac{1-2\nu}{8\pi(1-\nu)}\left(\frac{1-\nu}{1-2\nu}I_1 - \frac{\nu}{1-2\nu}(I_3 - I_2)\right) - \left.\frac{\nu}{1-2\nu}\right]\epsilon_{33}^*
\end{aligned} \tag{10}$$

$$\sigma_{12}/2\mu = \left(\frac{a_1^2 + a_2^2}{8\pi(1-\nu)}I_{12} + \frac{1-2\nu}{8\pi(1-\nu)}(I_1 + I_2) - 1\right)\epsilon_{12}^* \tag{11}$$

Rest of stress terms can be found out by taking a cyclic permutation of the above equations
Hence, the stresses are constant for inside points, and take negative values (**indicating compression**)

2.1.2 Exterior Points

The stress and strains here are not constant, hence have to be calculated at every point. This is done by calculating the induced strain at each point, using the D_{ijkl} tensor, and the given eigenstrain. We consider the following integrals for any exterior point with coordinates (x_1, x_2, x_3)(Similar to the one's used for interior points)

$$I_i = 2\pi a_1 a_2 a_3 \int_\lambda^\infty \frac{ds}{(a_i^2 + s)\Delta(s)} \tag{12}$$

$$I_{ii} = 2\pi a_1 a_2 a_3 \int_\lambda^\infty \frac{ds}{(a_i^2 + s)^2\Delta(s)} \tag{13}$$

$$I_{ij} = 2\pi a_1 a_2 a_3 \int_\lambda^\infty \frac{ds}{(a_i^2 + s)(a_j^2 + s)\Delta(s)} \tag{14}$$

where λ is the largest positive root of the equation:

$$\frac{x_1^2}{a_1^2+\lambda}+\frac{x_2^2}{a_2^2+\lambda}+\frac{x_3^2}{a_3^2+\lambda}=1 \tag{15}$$

The equations (10), (11), (12) can be estimated by using the elliptic integrals indicated in equation (4)

$\theta = \arcsin\frac{a_1^2-a_3^2}{a_1^2+\lambda}$ and $k=\left(\frac{a_1^2-a_2^2}{a_1^2-a_3^2}\right)^{1/2}$

Then the integrals are given by:

$$I_1(\lambda)=\frac{4\pi a_1a_2a_3}{(a_1^2-a_2^2)(a_1^2-a_3^2)^{\frac{1}{2}}}(F(\theta(\lambda),k)-E(\theta(\lambda),k)) \tag{16}$$

$$I_3(\lambda)=\frac{4\pi a_1a_2a_3}{(a_2^2-a_3^2)(a_1^2-a_3^2)^{\frac{1}{2}}}\left(\frac{(a_2^2+\lambda)(a_1^2-a_3^2)^{\frac{1}{2}}}{\prod_k(a_k^2+\lambda)^{\frac{1}{2}}}-E(\theta(\lambda),k)\right) \tag{17}$$

Rest of the integrals in equations (10), (11), (12) can be found out from the above 2 equations as:

$$I_2(\lambda)=\frac{4\pi a_1a_2a_3}{\prod_k(a_k^2+\lambda)^{\frac{1}{2}}} \tag{18}$$

$$I_{ij}(\lambda)=\frac{I_j(\lambda)-I_i(\lambda)}{a_i^2-a_j^2},\quad \text{For } i\neq j \tag{19}$$

Further, we have to calculate the derivatives of the above $I_i's$ and $I_{ij}'s$ For this, we need to define the derivative and double derivative of $\lambda(x)$, in the respective directions.
The first derivative along i is given by:

$$\lambda_{,i}=\frac{2x_i}{a_i^2+\lambda}\Big/\sum_j\frac{x_j^2}{a_j^2+\lambda} \tag{20}$$

Double derivative along ij is given by:
(By manual derivative calculation of above equation (18)

$$\lambda_{,ij}=\frac{F_{i,j}-\lambda_iC_j}{C} \tag{21}$$

Where, $F_i=\frac{2x_i}{a_i+\lambda}$, and hence $F_{ij}=\frac{-2x_i\lambda_{,j}}{(a_i^2+\lambda)^2}$

$C=\sum_i\frac{x_i^2}{(a_i^2+\lambda)^2}$ and hence, $C_j=-2\lambda_j\sum_i\frac{x_i^2}{(a_i^2+\lambda)^3}$

Now the derivatives of the integrals in equations (14), (15), (16), (17) can be found out as:

$$I_{i,j}=\frac{-2\pi a_1a_2a_3}{(a_i^2+\lambda)\Delta S}\lambda_{,j} \tag{22}$$

$$I_{ij,k}=\frac{-2\pi a_1a_2a_3}{(a_i^2+\lambda)(a_j^2+\lambda)\Delta S}\lambda_{,k} \tag{23}$$

$$I_{i,jk}=\frac{-2\pi a_1a_2a_3}{(a_i^2+\lambda)\Delta S}\left(\lambda_{,jk}-\left(\frac{1}{(a_i^2+\lambda)}+\frac{1}{2}T\right)\lambda_{,j}\lambda_{,k}\right) \tag{24}$$

$$I_{i,jk}=\frac{-2\pi a_1a_2a_3}{(a_i^2+\lambda)(a_j^2+\lambda)\Delta S}\left(\lambda_{,jk}-\left(\frac{1}{(a_i^2+\lambda)}+\frac{1}{(a_j^2+\lambda)}+\frac{1}{2}T\right)\lambda_{,j}\lambda_{,k}\right) \tag{25}$$

where, $T=\sum_n\frac{1}{(a_n^2+\lambda)}$ and $\Delta S=\prod_m(a_m^2+\lambda)^{\frac{1}{2}}$

After computing all elliptic integrals and their derivatives, the compliance or elasticity tensor S_{ijkl} can be found as:

$$\begin{aligned}8\pi(1-\nu)S_{ijkl}(\lambda)&=\delta_{ij}\delta_{kl}\left[2\nu I_I(\lambda)-I_K(\lambda)+a_I^2I_{KI}(\lambda)\right]\\&+(\delta_{ik}\delta_{jl}+\delta_{jk}\delta_{il})\left(a_I^2I_{IJ}(\lambda)-I_J(\lambda)+(1-v)\left[I_K(\lambda)+I_L(\lambda)\right]\right)\end{aligned} \tag{26}$$

where δ_{ij} is the Dirac's Kroneker Delta function.
Hence, now the D_{ijkl} tensor can be calculated as follows:

$$\begin{aligned}8\pi(1-\nu)D_{ijkl}(x) &= 8\pi(1-\nu)S_{ijkl}(\lambda) + 2\nu\delta_{kl}x_i I_{I,j}(\lambda) \\ &+ (1-\nu)\left[\delta_{il}x_k I_{K,j}(\lambda) + \delta_{jl}x_k I_{K,i}(\lambda) + \delta_{ik}x_l I_{L,j}(\lambda) + \delta_{jk}x_l I_{L,i}(\lambda)\right] \\ &- \delta_{ij}x_k\left[I_K(\lambda) - a_I^2 I_{KI}(\lambda)\right]_{,l} - (\delta_{ik}x_j + \delta_{jk}x_i)\left[I_J(\lambda) - a_I^2 I_{IJ}(\lambda)\right]_{,l} \\ &- (\delta_{il}x_j + \delta_{jl}x_i)\left[I_J(\lambda) - a_I^2 I_{IJ}(\lambda)\right]_{,k} - x_i x_j\left[I_J(\lambda) - a_I^2 I_{IJ}(\lambda)\right]_{,lk} \end{aligned} \tag{27}$$

Note: For interior points, $\lambda = 0$ and hence all derivatives are also 0. Hence, at these points, $S_{ijkl} = D_{ijkl}$

Hence, now the induced strain field outside can be found from the given eigenstrain using the following equation:

$$\epsilon_{ij} = D_{ijkl}\epsilon^*_{kl} \tag{28}$$

Further, by using Hooke's Law we can finally calculate the stress field for outside points

$$\sigma_{ij} = C_{ijkl}\epsilon_{kl} \tag{29}$$

where $C_{ijkl} = \lambda_0\delta_{ij}\delta_{kl} + \mu(\delta_{ik}\delta_{jl} + \delta_{il}\delta_{jk})$ is the elastic tensor.

Here, $\lambda_0 = \frac{2\mu\nu}{1-2\nu}$ and $\mu = \frac{E}{2(1+\nu)}$ are the Lame's constants

2.2 3D Isotropic In-homogeneous Case

In the above case, the elastic moduli for the inclusion and matrix were the same, whereas this is not the case in in-homogeneous case. The results are obtained by the **Equivalent Inclusion Method**. In this method, a strain ϵ^*_{ij} is introduced to simulate the stress due to the eigenstrain resulting from the inhomogeneous inclusion.
Suppose that an inclusion with elasticity C^*_{ijkl} is inside a matrix with elasticity C_{ijkl}. Then the condition for equivalency of strains in the in-homogeneous inclusion is:

$$C^*_{ijkl}(\epsilon^0_{kl} + \epsilon_{kl}) = C_{ijkl}(\epsilon^0_{kl} + \epsilon_{kl} - \epsilon^*_{kl}) \tag{30}$$

where ϵ^0_{kl} represents an applied macroscopic strain which may be applied to the overall composite material To solve for the fictitious eigenstrain ϵ^*_{ij}, we have the following:

$$(\Delta C_{ijkl}S_{klmn} - C_{ijmn})\epsilon^*_{mn} = -\Delta C_{ijkl}\epsilon^0_{kl} - C^*_{ijkl}\epsilon^p_{kl} \tag{31}$$

where, $\Delta C_{ijkl} = C_{ijkl} - C^*_{ijkl}$ and ϵ^p_{kl} is the eigenstrain that the inhomogeneity is subjected to. From here, we get the equations for strain and stress at the interior and exterior points. For interior points

$$\begin{aligned}\epsilon_{ij} &= \epsilon^0_{ij} + S_{ijkl}\epsilon^*_{kl} \\ \sigma_{ij} &= \sigma^0_{ij} + C_{ijkl}(S_{ijkl}\epsilon^0_{mn} - \epsilon^0_{mn})\end{aligned} \tag{32}$$

$$\begin{aligned}\epsilon_{ij}(x) &= \epsilon^0_{ij}(x) + D_{ijkl}(x)\epsilon^*_{kl} \\ \sigma_{ij}(x) &= \sigma^0_{ij} + C_{ijkl}D_{ijkl}(x)\epsilon^0_{mn}\end{aligned} \tag{33}$$

The equation (30) holds for interior points whereas equation (31) holds for exterior points, and in this way the stress fields can be calculated for this case.

3 Validation of Outputs

3.1 Homogeneous Case, Interior Points

These results were validated using the case by case outputs given in Mura (page 79 onwards)

$$\sigma_{11} = -\mu\frac{16}{15(1-\nu)}\epsilon^*_{11} - 2\mu\frac{5\nu+1}{15(1-\nu)}\epsilon^*_{22} - 2\mu\frac{5\nu+1}{15(1-\nu)}\epsilon^*_{33},$$
$$\sigma_{12} = -2\mu\frac{7-5\nu}{15(1-\nu)}\epsilon^*_{12}. \qquad (11.21.1)$$

All other stress components are obtained by the cyclic permutation of (1, 2, 3).

Figure 2: Sphere

- Sphere ($a_1 = a_2 = a_3$)
  Here, the stress fields are independent of the dimension of the sphere.
  Unit test: $E = 210, \nu = 0.3, \epsilon^*_{ii} = 0.001, \epsilon^*_{ij} = 0$
  Expected outputs from above formula:

$$\sigma = \begin{bmatrix} -0.200 & 0 & 0 \\ 0 & -0.200 & 0 \\ 0 & 0 & -0.200 \end{bmatrix}$$

  Output from code:

```
Stress =
[[-0.200000499973446 -0.0 -0.0]
 [-0.0 -0.199999999993248 -0.0]
 [-0.0 -0.0 -0.199999500033309]]
```

Figure 3: Sphere Output

Note that the slight deviation is due to the fact that the inputs cannot be given as an exact shpere, but have to be of the format $(10.0012, 10.0011, 10.001)$ which is an approximate sphere. This constraint is due to the presence of a_i in the denominator of formulae as in equation $(4), (5)$ etc

- Elliptic Cylinder ($a_1 \to \infty$)
  Unit test: $a_1 = 99999, a_2 = 3, a_3 = 1, E = 210, \nu = 0.3, \epsilon^*_{ii} = 0.001, \epsilon^*_{ij} = 0$
  Expected outputs from above formula:

$$\sigma = \begin{bmatrix} -0.3 & 0 & 0 \\ 0 & -0.225 & 0 \\ 0 & 0 & -0.075 \end{bmatrix}$$

  Output from code:

$$\sigma_{11} = \frac{\mu}{1-\nu}\left\{-2 + \frac{a_2^2 + 2a_1a_2}{(a_1+a_2)^2} + \frac{a_2}{a_1+a_2}\right\}\epsilon_{11}^* + \frac{\mu}{1-\nu}\left\{\frac{a_2^2}{(a_1+a_2)^2} - \frac{a_2}{a_1+a_2}\right\}\epsilon_{22}^* - \frac{2\mu\nu}{1-\nu}\frac{a_1}{a_1+a_2}\epsilon_{33}^*,$$

$$\sigma_{22} = \frac{\mu}{1-\nu}\left\{-2 + \frac{a_1^2 + 2a_1a_2}{(a_1+a_2)^2} + \frac{a_1}{a_1+a_2}\right\}\epsilon_{22}^* + \frac{\mu}{1-\nu}\left\{\frac{a_1^2}{(a_1+a_2)^2} - \frac{a_1}{a_1+a_2}\right\}\epsilon_{11}^* - \frac{2\mu\nu}{1-\nu}\frac{a_2}{a_1+a_2}\epsilon_{33}^*,$$

$$\sigma_{33} = \frac{-2\mu\nu}{1-\nu}\frac{a_1}{a_1+a_2}\epsilon_{11}^* - \frac{2\mu\nu}{1-\nu}\frac{a_2}{a_1+a_2}\epsilon_{22}^* - \frac{2\mu}{1-\nu}\epsilon_{33}^*,$$

$$\sigma_{12} = -\frac{2\mu}{1-\nu}\frac{a_1a_2}{(a_1+a_2)^2}\epsilon_{12}^*, \quad \sigma_{23} = -2\mu\frac{a_2}{a_1+a_2}\epsilon_{23}^*,$$

$$\sigma_{31} = -2\mu\frac{a_1}{a_1+a_2}\epsilon_{31}^*.$$

Figure 4: Elliptic Cylinder

```
Point is inside
[[-0.299999999053818 -0.0 -0.0]
 [-0.0 -0.225000000461840 -0.0]
 [-0.0 -0.0 -0.0750000004843401]]
```

Figure 5: Elliptic Cylinder Output

- Penny Shape ($a_1 = a_2 >> a_3$)

$$\sigma_{11}/2\mu = \frac{-\nu}{1-\nu}(\epsilon_{11}^* + \epsilon_{22}^*) - \epsilon_{11}^* + \frac{13}{32(1-\nu)}\frac{\pi a_3}{a_1}\epsilon_{11}^* + \frac{16\nu-1}{32(1-\nu)}\frac{\pi a_3}{a_1}\epsilon_{22}^* - \frac{2\nu+1}{8(1-\nu)}\frac{\pi a_3}{a_1}\epsilon_{33}^*,$$

$$\sigma_{22}/2\mu = \frac{-\nu}{1-\nu}(\epsilon_{11}^* + \epsilon_{22}^*) - \epsilon_{22}^* + \frac{16\nu-1}{32(1-\nu)}\frac{\pi a_3}{a_1}\epsilon_{11}^* + \frac{13}{32(1-\nu)}\frac{\pi a_3}{a_1}\epsilon_{22}^* - \frac{2\nu+1}{8(1-\nu)}\frac{\pi a_3}{a_1}\epsilon_{33}^*, \tag{11.23.1}$$

$$\sigma_{33}/2\mu = -\frac{2\nu+1}{8(1-\nu)}\frac{\pi a_3}{a_1}\epsilon_{11}^* - \frac{2\nu+1}{8(1-\nu)}\frac{\pi a_3}{a_1}\epsilon_{22}^* - \frac{1}{4(1-\nu)}\frac{\pi a_3}{a_1}\epsilon_{33}^*,$$

$$\sigma_{23}/2\mu = \frac{\nu-2}{4(1-\nu)}\frac{\pi a_3}{a_1}\epsilon_{23}^*, \quad \sigma_{31}/2\mu = \frac{\nu-2}{4(1-\nu)}\frac{\pi a_3}{a_1}\epsilon_{31}^*,$$

$$\sigma_{12}/2\mu = -\epsilon_{12}^* + \frac{7-8\nu}{16(1-\nu)}\frac{\pi a_3}{a_1}\epsilon_{12}^*;$$

Figure 6: Penny Shape

Unit test: $a_1 = 20, a_2 = 19.999, a_3 = 0.001, E = 210, \nu = 0.3,$
$\epsilon_{ii}^* = 0.001, \epsilon_{ij}^* = 0$

Expected outputs from above formula:

$$\sigma = \begin{bmatrix} -0.29996 & 0 & 0 \\ 0 & -0.29996 & 0 \\ 0 & 0 & -2.3\text{x}10^{-5} \end{bmatrix}$$

Output from code:

```
Stress =
[[-0.299988219924772 -0.0 -0.0]
 [-0.0 -0.299988219041230 -0.0]
 [-0.0 -0.0 -2.35610339959652e-5]]
```

Figure 7: Penny Shape Output

Note: In all of the above cases, the answers have errors in the 3rd-4th decimal place. This is due to the input constraints we have to give which are the following: $a_1 > a_2 > a_3$; $a_1 \neq a_2 \neq a_3$

3.2 In-homogeneous Case, Inside Points

The results were validated using the ϵ (final strain) outputs given in Mura (pg 183 onwards)

- Sphere

From (11.15) and (11.21), ϵ_{ij} inside the spherical inclusion with uniform eigenstrains ϵ_{11}^{**}, ϵ_{22}^{**} and ϵ_{33}^{**} are given by

$$\begin{aligned} 15(1-\nu)\epsilon_{11} &= (7-5\nu)\epsilon_{11}^{**} + (5\nu-1)\epsilon_{22}^{**} + (5\nu-1)\epsilon_{33}^{**}, \\ 15(1-\nu)\epsilon_{22} &= (5\nu-1)\epsilon_{11}^{**} + (7-5\nu)\epsilon_{22}^{**} + (5\nu-1)\epsilon_{33}^{**}, \\ 15(1-\nu)\epsilon_{33} &= (5\nu-1)\epsilon_{11}^{**} + (5\nu-1)\epsilon_{22}^{**} + (7-5\nu)\epsilon_{33}^{**}, \end{aligned} \tag{22.21}$$

Figure 8: Sphere

Unit test: $E = 210, \nu = 0.3, \epsilon_{ii}^{p} = 0.001, \epsilon_{ij}^{p} = 0$
From this, we get the uniform eigenstrains $\epsilon_{ii}^{**} = 0.001$
Expected values of ϵ from above equation:

$$\epsilon_{11} = \epsilon_{22} = \epsilon_{33} = 0.00061 \tag{34}$$

Output from code:

```
EPSILON
[[0.00061902 0.         0.        ]
 [0.         0.00061905 0.        ]
 [0.         0.         0.00061908]]
```

Figure 9: Sphere output

- Penny Shape

When Ω is a penny-shaped inhomogeneity, $a_1 = a_2 = a$ and $a_3 = 0$. From (11.23), ϵ_{ij} inside Ω, for given ϵ_{11}^{**}, ϵ_{22}^{**} and ϵ_{33}^{**}, are

$$\epsilon_{11} = \epsilon_{22} = 0, \quad \epsilon_{33} = \epsilon_{11}^{**}\nu/(1-\nu) + \epsilon_{22}^{**}\nu/(1-\nu) + \epsilon_{33}^{**}. \tag{22.27}$$

Figure 10: Penny Shape

Unit test: $a_1 = 20, a_2 = 19.999, a_3 = 0.001, E = 210, \nu = 0.3,$

$\epsilon^p_{ii} = 0.001, \epsilon^p_{ij} = 0$
From this, we get the uniform eigenstrains $\epsilon^{**}_{ii} = 0.001$
Expected values from above equation

$$\epsilon_{11} = \epsilon_{22} = 0, \epsilon_{33} = 0.0018 \tag{35}$$

Output from code:

```
EPSILON
[[7.29242752e-08 0.00000000e+00 0.00000000e+00]
 [0.00000000e+00 7.29297448e-08 0.00000000e+00]
 [0.00000000e+00 0.00000000e+00 1.85699700e-03]]
```

Figure 11: Penny Shape output

3.3 Outside Points

The partial validation was done by referring to similar graph's from Prof. Gururajan's thesis.

Graph for Spherical Inclusion (σ_{ii} along x axis)

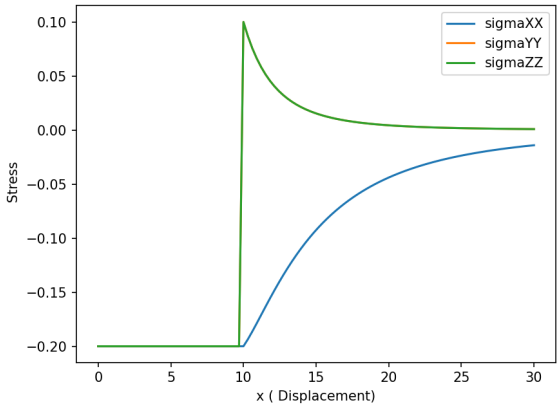

Figure 12: Code output for a sphere

The above graph should have trace of the σ matrix to be 0 for outside points. As of now, we are getting the trace error to be between 0 and 5 percent, with the higher error being at points just outside the inclusion.

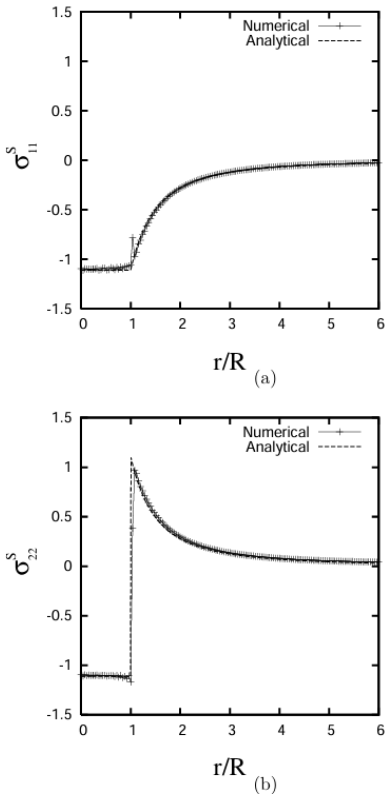

Figure 13: Thesis graph

4 Graphical User Interface (GUI)

4.1 Introduction

Institutional scientific research often demands sophisticated tools to analyze data, visualize results, and facilitate experimentation. To address this need, we have developed a comprehensive Graphical User Interface (GUI) application utilizing advanced technologies. This report outlines the design, development, and functionality of the application, emphasizing its significance in scientific research within our institution.

4.2 Technologies Utilized

The application leverages a stack of cutting-edge technologies to ensure efficiency and versatility:

4.2.1 Backend Development

Node.js and Express.js frameworks are employed for robust backend development, enabling seamless data processing and communication.

4.2.2 Frontend Development

Electron.js is utilized for frontend development, offering a cross-platform desktop application framework that integrates seamlessly with Node.js.

4.2.3 Scientific Plotting Library

Mayavi, a powerful library for 3D scientific data visualization, is integrated to provide sophisticated plotting capabilities essential for research analysis.

4.2.4 Python Libraries

Numpy and Pandas are utilized for numerical computing and data manipulation, augmenting the application's analytical capabilities.

4.2.5 Web Technologies

HTML, CSS, and JavaScript are employed to design an intuitive and user-friendly interface, enhancing the accessibility and usability of the application.

4.3 Key Features

The GUI application boasts an array of features tailored to meet the diverse requirements of scientific research:

4.3.1 Data Visualization

Utilizing Mayavi, the application enables users to visualize complex scientific data in three dimensions, facilitating a deeper understanding of research findings.

4.3.2 Data Analysis

Leveraging Python libraries such as Numpy and Pandas, the application offers robust data analysis capabilities, empowering researchers to extract valuable insights from their data.

4.3.3 Customization

The application provides extensive customization options, allowing users to tailor visualizations and analyses to suit their specific research requirements.

4.3.4 User Interface

The intuitive and user-friendly interface, developed using HTML, CSS, and JavaScript, enhances user experience and facilitates efficient navigation and interaction with the application.

4.4 Implementation Details

The application is implemented following a modular and scalable architecture, ensuring maintainability and extensibility. The backend functionalities are implemented using Node.js and Express.js, providing a robust foundation for data processing and communication. The frontend interface is developed using Electron.js, facilitating seamless integration with the backend and enabling desktop application deployment. Python scripts utilizing Numpy and Pandas are integrated into the backend to handle complex data analysis tasks, while Mayavi is utilized for advanced 3D visualization.

4.5 Conclusion

The development of this GUI application represents a significant advancement in our institution's scientific research capabilities. By harnessing advanced technologies such as Node.js, Electron.js, and Mayavi, we have created a versatile tool that empowers researchers to conduct complex data analysis and visualization with ease. The intuitive interface and extensive features ensure accessibility and usability across various research domains, contributing to the advancement of scientific knowledge within our institution.

4.6 Future Enhancements

Future enhancements to the application may include:

- Integration of additional scientific libraries for enhanced functionality.
- Implementation of collaborative features to facilitate teamwork and data sharing.
- Optimization of performance and scalability to handle larger datasets efficiently.

4.7 Acknowledgements

We extend our sincere appreciation to all individuals who contributed to the development and implementation of this project, from conceptualization to execution. We would like to thank our guide Prof. Gururajan for introducing and guiding us through the problem. We would also like to thank Prof. Ramachandran, who has written the open source software Mayavi, which we have used for visualization.

5 References

- T. Mura. *Micromechanics of Defects in Solids. Mechanics of Elastic and Inelastic Solids.* Springer Netherlands, 1987.
- M. Gururajan. *Elastic Inhomogeneity Effects on Microstructures : A Phase Field Study (PhD thesis).* 01 2006
- Chris Weinberger and Wei Cai. Lecture note 2. eshelby's inclusion i. *ME340B– Elasticity of Microscopic Structures– Stanford University, Wi*n ter 2004, page 2:5, 2004.
- https://github.com/cmeg2022/Raj/blob/main/DDP
- https://www.sciencedirect.com/science/article/pii/S0098300411002378